Published in final edited form as:
Int J Radiat Oncol Biol Phys. 2008 October 1; 72(2): 610–616. doi:10.1016/j.ijrobp.2008.06.1488.

Evaluation of multiple breathing states using a multiple instance geometry approximation (MIGA) in inverse-planned optimization for loco-regional breast treatment

Alexander Lin, M.D., **Jean M. Moran, Ph.D.**, **Robin B. Marsh, C.M.D.**, **James M. Balter, Ph.D.**, **Benedick A. Fraass, Ph.D.**, **Daniel L. McShan, Ph.D.**, **Marc L. Kessler, Ph.D.**, and **Lori J. Pierce, M.D.**
Department of Radiation Oncology, University of Michigan, Ann Arbor, Michigan, U.S.A

Abstract

Purpose—Although previous work demonstrated superior dose distributions for left-sided breast cancer patients planned for IMRT at deep inspiration breath hold compared to conventional techniques with free-breathing, it is not always feasible to use such techniques to limit the impact of respiration on treatment delivery. This study assesses whether optimization based on multiple instance geometry approximation (MIGA) can derive an IMRT plan that is less sensitive to known respiratory motions.

Methods and Materials—CT scans were acquired with an active breathing control (ABC) device at multiple breathhold states. Three inverse optimized plans were generated for 8 left-sided breast cancer patients: one static IMRT plan optimized at end exhale, and 2 (MIGA) plans based on a MIGA representation of normal breathing, and a MIGA representation of deep breathing, respectively. Breast and nodal targets were prescribed 52.2 Gy and a simultaneous tumor bed boost was prescribed 60 Gy.

Results—With normal breathing, doses to the targets, heart, and LAD were equivalent whether optimizing with MIGA or on a static dataset. When simulating motion due to deep breathing, optimization with MIGA appears to yield superior tumor bed coverage, decreased LAD mean dose, and maximum heart and LAD dose when compared to optimization on a static representation.

Conclusions—For left-sided breast-cancer patients, inverse-based optimization accounting for motion due to normal breathing may be similar to optimization on a static dataset. However, some patients may benefit from accounting for deep breathing with MIGA with improvements in tumor bed coverage and dose to critical structures.

Keywords

Breast cancer; Locoregional radiation; IMRT; Inverse optimization; Motion

Corresponding Author: Lori J. Pierce, M.D. University of Michigan, Department of Radiation Oncology, 1500 East Medical Center Drive, UH B2C490, Box 0010, Ann Arbor, MI 48109-0010 Telephone: 734-936-4300 Fax: 734-763-7370 Email: ljpierce@med.umich.edu.

Conflict of Interest Notification
All authors report no actual or potential conflicts of interest.

Introduction

Radiotherapy plays a key role in the management of breast cancer patients following either breast-conserving therapy (BCT) or mastectomy. Several studies randomizing patients to postmastectomy radiotherapy have demonstrated a benefit in overall survival [1–3]. A recent update of the Overview by the Early Breast Cancer Trialists' Collaborative Group (EBCTG) meta-analysis of all randomized trials demonstrates a statistically significant improvement in overall survival with radiotherapy following BCT or mastectomy [4].

Despite a proven survival benefit and contemporary radiotherapy techniques, treatment, especially for patients requiring left-sided locoregional radiation, can result in significant toxicity. Radiation-associated heart disease can manifest in a spectrum of clinical diagnoses such as pericarditis, pancarditis, cardiomyopathy, and coronary artery disease, with cardiac ischemia of greatest clinical significance [5]. Recent studies show delivery of high doses to small regions of the left anterior heart [6] as well as an increase in cardiac events following left-sided radiotherapy compared to right-sided treatment [7]. The updated EBCTG meta-analysis demonstrated a statistically significant excess heart disease mortality risk in women receiving radiotherapy [4]. Based on these data, radiotherapy techniques that minimize dose delivered to the heart and vessels are important.

Intensity Modulated Radiation Therapy (IMRT) is a treatment delivery technique that utilizes computer-based inverse planning optimization to modulate the intensities of individual beamlets. It offers the ability to define targets and normal tissues, and to specify with what flexibility target coverage and tissue sparing can be obtained. Although little data exists on IMRT for breast cancer patients requiring nodal RT, a potential advantage more easily achieved with IMRT may be to decrease the doses delivered to critical normal structures, while maintaining adequate target coverage.

Difficulties associated with breast treatment include respiratory motion as well as the proximity of the heart to the radiotherapy targets. An active breathing control (ABC) device has been used as a means in left-sided breast cancer patients receiving radiotherapy to fix the respiratory state, which if done at deep inspiration breath hold (DIBH), can reduce the volume of heart irradiated [8]. With the ABC device, motion uncertainties due to breathing can be minimized by delivering treatment at a predefined, reproducible breath hold state. Previous studies have investigated the impact of ABC at normal inhale, exhale, and DIBH to reduce the dose to lungs and/or heart for breast cancer patients [8–10].

It is not always feasible, however, to use devices such as an ABC device to limit the impact of respiration on treatment delivery. Potential disadvantages of using such a device include its lack of availability in most clinics as well as prolonged treatment time, as well as the fact that a fraction of patients can only tolerate very short breath holds, making use of the ABC device inappropriate. A technique that could deliver an equally conformal plan with less intervention and shorter treatment times would therefore be a promising option.

IMRT plans that are optimized to be highly conformal based on static patient geometry can be degraded by intra-treatment motion [11,12]. In order to achieve an optimal IMRT plan in the face of geometric uncertainty from breathing, we have utilized a simulation of multiple instances of patient geometry to account for motion uncertainties. The Multiple Instances of Geometry Approximation (MIGA) approach [13] has been used here to develop IMRT plans that are robust to the patient's respiratory motion. This study assesses whether optimization using MIGA results in IMRT plans that are less sensitive to known respiratory motions during beam delivery for locoregional radiation to left-sided breast cancer patients.

Methods and Materials

Patients and Pre-planning Procedures

For this IRB approved study, CT scans were obtained for 8 patients with left-sided breast cancer who required loco-regional radiotherapy after being treated with breast conservation (lumpectomy and axillary lymph node dissection). CT scans were acquired with patients positioned supine on a carbon fiber breast board with above the head arm rests with indexed positions (Sinmed BV, The Netherlands). Scans of the immobilized patient were obtained using 3–5 mm-thick slices from the upper neck, above the thyroid notch, to the upper abdomen. An ABC device (vMax, Sensormedics, Yorba Linda, CA) was used to control breath hold and CT datasets were obtained at breathing states of end exhale, 20%, 40%, 60%, and 80% vital capacity. CT data were then input into the 3-D treatment planning system ("UMPlan") that has been developed at our institution [14,15]

Target and normal structure definition

Targets and organs at risk were identified and contoured on the axial CT images. The primary target volumes included the ipsilateral breast, the operative tumor bed, and the supraclavicular, infraclavicular, and internal mammary (limited to the first 3 intercostal spaces) lymph node chains. Nodal volumes were defined based on published findings from our institution [16]. The ipsilateral breast CTV was defined on each axial slice, based on the anatomic borders of the breast and consisted of the breast volume that would be treated with standard tangents. A buildup region extending from the breast surface to a depth of 5 mm was excluded from the breast CTV. The tumor bed CTV was contoured based on the extent defined by the post-operative changes as well as the operative markers placed at time of lumpectomy. Based on our previous investigations, CTVs were expanded to create PTVs to account for the average motion and reproducibility of target positioning using ABC [17]. Organs at risk which were contoured included the heart, the left anterior descending artery (LAD), great vessels, ipsilateral lung, brachial plexus, and carotid artery. Brachial plexus, heart, and LAD were defined based on methods published by our institution [16,18]. For each patient, the target and normal tissue movement at 20%, 40%, 60%, and 80% vital capacity with respect to the end exhale scan were determined using a mutual information-based regional rigid alignment[17]. Alignment to the end-exhale state was performed using a three-dimensional regional rigid alignment tool for rotation and translation developed at the Netherlands Cancer Institute [19]. Review of each alignment was performed on axial, coronal, and sagittal planes, and the displacements of targets and critical structures at each breath hold state relative to end exhale were then determined.

Treatment Planning

Three plans were generated for each patient.

1. A static IMRT plan optimized on the end exhale state, with ABC for controlled breath hold (STATIC-EXHALE)
2. A MIGA-based IMRT plan optimized to 3 geometric instances (end exhale, 20%, and 40% of vital capacity), which represents the range of a normal breathing cycle (MIGA-NORMAL-RESP)
3. A MIGA-based IMRT plan optimized to 5-geometric instances (end exhale, 20%, 40%, 60%, and 80% of vital capacity) which represents the range of a deep breathing cycle (MIGA-DEEP-RESP)

For the MIGA plans, the temporal weighting of each simulated phase of breathing (breath hold state) was determined from patient-specific breathing cycle traces obtained at the time of

simulation (Varian, RPM system, Palo Alto, CA). These datasets were then used to describe rigid body translations/rotations, as described above.

The total number of beams used for each plan ranged from three to five. Beam energies of 6 and 16 MV were used, depending on the patient geometry. For each individual patient, the same beam arrangement and energies were used across the 3 separate optimized plans. Dose to the contralateral breast and lung was restricted to scatter and transmission dose by preventing beams from entering or exiting these defined structures.

The same cost function was used for all patients and treatment plans. A simultaneous boost technique was used: the breast, supraclavicular, infraclavicular, and IMNs were prescribed 52.2 Gy in 1.74 Gy fractions (equivalent to 50 Gy in 2 Gy fractions) and the tumor bed was prescribed 60 Gy, all delivered in 30 fractions. The heart and left anterior descending artery (LAD) were limited to a mean dose of 3 Gy, and a maximum dose of 15 Gy. No more than 30% of the ipsilateral lung was permitted to exceed 20 Gy. The highest priority for optimization was placed on target coverage, followed by heart and LAD constraints. Complete dose specifications and planning priorities are listed in Table 1.

To represent the expected doses delivered by the static plan on a breathing patient, the static-derived IMRT plan (end exhale) was also applied to the normal (3-states) and deep respiration (5-states) MIGA geometries. The expected dose distributions for each of these plans were then calculated on the MIGA anatomical representations created with the same frequencies and instances used for the MIGA-optimized plans. These data were then compared to dose distributions obtained for normal and deep respiration by the patients, optimized on the appropriate MIGA-based anatomy (see Table 2). All dose distributions were calculated with density correction using a convolution/superposition method based on work by Mackie et al. [20].

Results

Dose-volume histograms were generated for all targets and organs at risk. Mean dose and minimum dose (to 1% of the volume) delivered to the targets were chosen as the metrics for target coverage comparisons. Mean dose and maximum dose (to 1% of the volume) were used to evaluate doses to the heart and LAD. Lung V20 (% volume of the ipsilateral lung receiving ≥ 20 Gy) and mean lung dose were used as comparison metrics for the ipsilateral lung, as these parameters are potentially indicative of the risk of developing pneumonitis in patients with breast cancer who have received radiotherapy [21–23]. Dose distributions were simulated for the following scenarios:

1. A static IMRT plan optimized on the end exhale state, delivered to a patient immobilized at end exhale.
2. A static IMRT plan optimized on the end exhale state, delivered to a patient breathing up to mid respiration (40% of vital capacity).
3. A static IMRT plan optimized on the end exhale state, delivered to a patient breathing up to deep respiration (up to 80% of vital capacity).
4. A MIGA-based IMRT plan, optimized to 3-geometric instances representing normal breathing (mid respiration, up to 40%), delivered on a patient undergoing normal respiration.
5. A MIGA-based IMRT plan, optimized to 5-geometric instances representing deep breathing (up to 80%), delivered on a patient undergoing deep respiration.

The mean, minimum, and maximum doses as well as the standard deviation for these parameters were computed for each structure of interest and for all treatment plans. A paired two-tailed t-test was used to compare values among the treatment-planning techniques. Statistical significance was set at a value of $p < 0.05$.

Doses delivered by a static IMRT plan on a breathing patient

Mean doses to targets and normal structures were calculated for the static-based IMRT plans delivered to end exhale, with normal breathing, and with deep breathing. While coverage of targets was not significantly altered with normal breathing, there was significant degradation observed in the average mean and maximum doses to the heart and LAD, as well as mean ipsilateral lung dose with deep breathing (Table 3).

MIGA-based optimization

MIGA-based optimization was then compared to static-based optimization for both normal breathing and deep breathing. When averaged over all patients, a MIGA-optimized plan that accounts for normal breathing did not significantly change the minimum or mean doses delivered to the targets when compared to optimization to the end exhale state (Table 4). The same was also found for critical normal structures, with no significant differences in mean doses to the lung, heart, or LAD, or maximum doses to the heart or LAD (Table 4).

With MIGA-based optimization simulating deep breathing, the MIGA-optimized plans demonstrated significantly better coverage of the tumor bed compared to the static-optimized plan with respect to minimum dose (57.9 ± 2 Gy vs. 55.4 ± 2.3 Gy, $p = 0.04$). Coverage of the remainder of the targets was otherwise similar between the two optimization techniques (Table 5). Superior sparing of the heart and LAD was demonstrated with optimization accounting for deep breathing (Table 5). Significant sparing was noted in maximum heart dose (10.5 ± 8.5 Gy vs. 13.5 ± 9 Gy, $p = 0.02$), maximum LAD dose (11.9 ± 6.2 Gy vs. 17.4 ± 7.7 Gy, p), and mean LAD dose (2.6 ± 2 vs. 3.5 ± 2.4 Gy, $p = 0.01$).

Although doses to targets and normal structures appeared equivalent when averaged over all patients between static-based optimization and MIGA-based optimization for normal breathing, individual patient data show measurable differences favoring MIGA, particularly in doses to the heart and LAD (Figures 1 and 2). Differences were most pronounced and significant for patients exhibiting deep breathing during treatment as described above, but were also evident for multiple patients with normal breathing.

Discussion

To our knowledge, this study is the first evaluation of robust IMRT optimization for breathing in left-sided breast cancer patients requiring locoregional radiotherapy. Patient breathing during treatment delivery can degrade IMRT optimization by requiring larger CTV to PTV margins compared to those for a patient treated in the absence of such motion [24], so we have hypothesized that using a multiple instance of geometry approximation (MIGA) during plan optimization to account for patient breathing could lead to improvements in inverse planning by compensating for the degradation of the plan caused by intra-treatment motion. A recent publication from our institution showed these benefits with MIGA when applied to a complex head and neck IMRT case considering setup error [13]. In the current work, the data show that static-based optimization degrades with motion due to breathing, and that deep breathing compromises treatment delivery more than normal breathing. Additionally, it was demonstrated that MIGA-based optimization can improve tumor bed coverage and reduce dose to the heart and LAD compared to static-based plans delivered with deep breathing, and that MIGA- based optimization can yield robust treatment plans which account for breathing during

treatment. With the larger displacement associated with deep breathing, the data in this work predict the realization of improvements in dose distributions when accounting for this uncertainty.

The role of locoregional radiation for patients with node-positive breast cancer is well-established, with a proven benefit in overall survival [1–4]. However, the long-term survival benefit comes at the potential cost of increased cardiovascular complications [5–7] from dose delivered to the heart and its associated vascular structures. This is especially relevant to left-sided breast cancer patients, where treatment of the locoregional nodes, particularly the internal mammary nodes, can add significant dose to the heart. The emergence of IMRT as a means to potentially improve treatment conformality offers the possibility of reducing the dose delivered to critical structures and the associated long-term treatment-related morbidity and mortality. Until recently, most clinical use of IMRT for breast treatment has been limited to breast-only radiation. Recently published techniques have included treatment of the supraclavicular and axillary lymph nodes[25,26]. Furthermore, planning comparison studies have shown that delivery of IMRT to the locoregional nodes, including the internal mammary nodes, significantly decreases the heart dose when compared to standard 3-D conformal techniques [27].

In patients treated with normal breathing, MIGA-based plans yielded equivalent results to the static-derived IMRT plan. This suggests that if patients can control and maintain shallow breathing during treatment, static-derived IMRT plans are robust to breathing motion. This is consistent with previous findings [9,28], and is most likely due to the small magnitude of target and critical structure displacement during normal breathing. However, examination of individual patient data supports the possibility that clinically important gains in reduction of dose to the heart or LAD (Fig. 2,3) may be realized for individuals when motion due to normal breathing is taken into account for optimization. We recommend identifying patients prospectively at the time of simulation for whom respiratory motion may be of concern, and to institute a method for respiratory motion management for these patients [29].

There are several potential advantages to using the multiple instance of geometry approximation in optimization. Combining the use of intensity modulation with an increased number of beams and with ABC adds complexity and time to treatment delivery. Other drawbacks to ABC include an inability of some patients to tolerate its use, as well as the fact that access to and training in the technique are not available in all treatment centers. In this study, we have shown that using MIGA-based optimization to account for breathing motion may yield significant benefits with respect to target coverage as well as sparing of critical tissues such as the heart and LAD. These benefits seem to be limited mostly to patients who breathe deeply during treatment, but patients may exist whose anatomy and motion with normal breathing may lead to an increased delivered dose to the heart or LAD than originally planned.

This study demonstrates the feasibility of using multiple geometry approximations to account for respiratory motion secondary to breathing. However, there are several limitations to our present analysis. The study was limited with respect to patient numbers, and the data represent calculated doses, and not actual delivered doses. Additionally, the optimization in this work used rigid body translations to represent changes in patient geometry rather than a deformation between the known breathing states. The inclusion of anatomic distortion when mapping between instances may be a more accurate representation of target and critical structure movement. Addressing geometric deformation and prospectively identifying patients who would benefit most from respiratory motion control will be the topics of further investigations using the MIGA optimization method for treatment of locoregional breast cancer patients.

Conclusions

This work shows that simulation of multiple instances of patient anatomy within the inverse planning process can help yield robust treatment plans that adequately cover targets while sparing critical structures. For patients who normally breathe to approximately 40% of vital capacity, MIGA-based optimization resulted in lower maximum heart and LAD doses for some patients while other patients did not seem to benefit. However, for patients who breathe more deeply (up to 80% vital capacity), MIGA-based optimization yields superior target coverage and tissue sparing. Further work needs to be done to address the broader question of whether the MIGA-based optimization method can fully compensate for motion in those patients who cannot tolerate the use of ABC during their treatments for breast cancer.

Acknowledgements

Presented in part at the 48th Annual Meeting of the American Society for Therapeutic Radiology and Oncology (ASTRO), Philadelphia, PA, November 5–9, 2006. Work supported by NIH R01-CA102435-01 and P01-CA59827.

References

1. Overgaard M, Hansen PS, Overgaard J, et al. Postoperative radiotherapy in high-risk premenopausal women with breast cancer who receive adjuvant chemotherapy. Danish Breast Cancer Cooperative Group 82b Trial. N Engl J Med 1997;337:949–955. [PubMed: 9395428]
2. Overgaard M, Jensen MB, Overgaard J, et al. Postoperative radiotherapy in high-risk postmenopausal breast-cancer patients given adjuvant tamoxifen: Danish Breast Cancer Cooperative Group DBCG 82c randomised trial. Lancet 1999;353:1641–1648. [PubMed: 10335782]
3. Ragaz J, Olivotto IA, Spinelli JJ, et al. Locoregional radiation therapy in patients with high-risk breast cancer receiving adjuvant chemotherapy: 20-year results of the British Columbia randomized trial. J Natl Cancer Inst 2005;97:116–126. [PubMed: 15657341]
4. Clarke M, Collins R, Darby S, et al. Effects of radiotherapy and of differences in the extent of surgery for early breast cancer on local recurrence and 15-year survival: an overview of the randomised trials. Lancet 2005;366:2087–2106. [PubMed: 16360786]
5. Corn BW, Trock BJ, Goodman RL. Irradiation-related ischemic heart disease. J Clin Oncol 1990;8:741–750. [PubMed: 2179483]
6. Fuller SA, Haybittle JL, Smith RE, et al. Cardiac doses in post-operative breast irradiation. Radiother Oncol 1992;25:19–24. [PubMed: 1410585]
7. Paszat LF, Mackillop WJ, Groome PA, et al. Mortality from myocardial infarction following postlumpectomy radiotherapy for breast cancer: a population-based study in Ontario, Canada. Int J Radiat Oncol Biol Phys 1999;43:755–762. [PubMed: 10098430]
8. Sixel KE, Aznar MC, Ung YC. Deep inspiration breath hold to reduce irradiated heart volume in breast cancer patients. Int J Radiat Oncol Biol Phys 2001;49:199–204. [PubMed: 11163515]
9. Frazier RC, Vicini FA, Sharpe MB, et al. Impact of breathing motion on whole breast radiotherapy: a dosimetric analysis using active breathing control. Int J Radiat Oncol Biol Phys 2004;58:1041–1047. [PubMed: 15001243]
10. Remouchamps VM, Vicini FA, Sharpe MB, et al. Significant reductions in heart and lung doses using deep inspiration breath hold with active breathing control and intensity-modulated radiation therapy for patients treated with locoregional breast irradiation. Int J Radiat Oncol Biol Phys 2003;55:392–406. [PubMed: 12527053]
11. Gierga DP, Chen GT, Kung JH, et al. Quantification of respiration-induced abdominal tumor motion and its impact on IMRT dose distributions. Int J Radiat Oncol Biol Phys 2004;58:1584–1595. [PubMed: 15050340]
12. Schwarz M, Van der Geer J, Van Herk M, et al. Impact of geometrical uncertainties on 3D CRT and IMRT dose distributions for lung cancer treatment. Int J Radiat Oncol Biol Phys 2006;65:1260–1269. [PubMed: 16798418]

13. McShan DL, Kessler ML, Vineberg K, et al. Inverse plan optimization accounting for random geometric uncertainties with a multiple instance geometry approximation (MIGA). Med Phys 2006;33:1510–1521. [PubMed: 16752585]
14. Lichter AS, Sandler HM, Robertson JM, et al. Clinical Experience With Three-Dimensional Treatment Planning. Semin Radiat Oncol 1992;2:257–266. [PubMed: 10717042]
15. McShan DL, Fraass BA, Lichter AS. Full integration of the beam's eye view concept into computerized treatment planning. Int J Radiat Oncol Biol Phys 1990;18:1485–1494. [PubMed: 2370198]
16. Madu CN, Quint DJ, Normolle DP, et al. Definition of the supraclavicular and infraclavicular nodes: implications for three-dimensional CT-based conformal radiation therapy. Radiology 2001;221:333–339. [PubMed: 11687672]
17. Moran JM, Balter JM, Ben-David MA, et al. Short-term displacement and reproducibility of the breast and nodal targets under active breathing control. Int J Radiat Oncol Biol Phys 2007;68:541–546. [PubMed: 17498569]
18. Krueger EA, Schipper MJ, Koellin T, et al. Cardiac chamber and coronary artery doses associated with postmastectomy radiotherapy techniques to the chest wall and regional nodes. Int J Radiat Oncol Biol Phys 2004;60:1195–1203. [PubMed: 15519792]
19. Wolthaus JW, van Herk M, Muller SH, et al. Fusion of respiration-correlated PET and CT scans: correlated lung tumour motion in anatomical and functional scans. Phys Med Biol 2005;50:1569–1583. [PubMed: 15798344]
20. Mackie TR, Bielajew AF, Rogers DW, et al. Generation of photon energy deposition kernels using the EGS Monte Carlo code. Phys Med Biol 1988;33:1–20. [PubMed: 3353444]
21. Lind PA, Wennberg B, Gagliardi G, et al. ROC curves and evaluation of radiation-induced pulmonary toxicity in breast cancer. Int J Radiat Oncol Biol Phys 2006;64:765–770. [PubMed: 16257129]
22. Seppenwoolde Y, Lebesque JV, de Jaeger K, et al. Comparing different NTCP models that predict the incidence of radiation pneumonitis. Normal tissue complication probability. Int J Radiat Oncol Biol Phys 2003;55:724–735. [PubMed: 12573760]
23. Rancati T, Wennberg B, Lind P, et al. Early clinical and radiological pulmonary complications following breast cancer radiation therapy: NTCP fit with four different models. Radiother Oncol 2007;82:308–316. [PubMed: 17224197]
24. George R, Keall PJ, Kini VR, et al. Quantifying the effect of intrafraction motion during breast IMRT planning and dose delivery. Med Phys 2003;30:552–562. [PubMed: 12722807]
25. Krueger EA, Fraass BA, McShan DL, et al. Potential gains for irradiation of chest wall and regional nodes with intensity modulated radiotherapy. Int J Radiat Oncol Biol Phys 2003;56:1023–1037. [PubMed: 12829138]
26. Chui CS, Hong L, McCormick B. Intensity-modulated radiotherapy technique for three-field breast treatment. Int J Radiat Oncol Biol Phys 2005;62:1217–1223. [PubMed: 15990027]
27. Thilmann C, Sroka-Perez G, Krempien R, et al. Inversely planned intensity modulated radiotherapy of the breast including the internal mammary chain: a plan comparison study. Technol Cancer Res Treat 2004;3:69–75. [PubMed: 14750895]
28. Thilmann C, Haring P, Thilmann L, et al. The influence of breathing motion on intensity modulated radiotherapy in the step-and-shoot technique: phantom measurements for irradiation of superficial target volumes. Phys Med Biol 2006;51:N117–126. [PubMed: 16510947]
29. Keall PJ, Mageras GS, Balter JM, et al. The management of respiratory motion in radiation oncology report of AAPM Task Group 76. Med Phys 2006;33:3874–3900. [PubMed: 17089851]

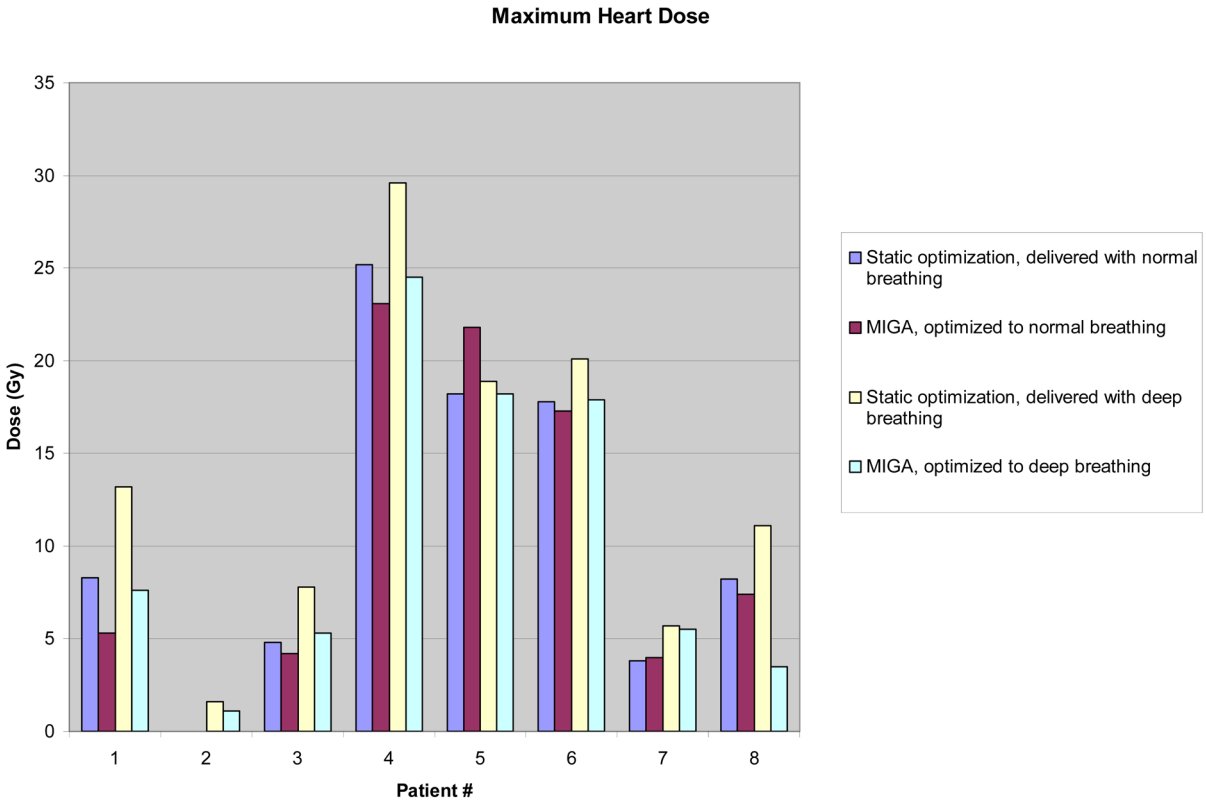

Figure 1.
Individual Patient Data for Maximum Heart Dose, comparing static vs MIGA-based optimization at both normal and deep breathing.
Abbreviations: MIGA, Multiple Instance Geometry Approximation; Gy, Gray

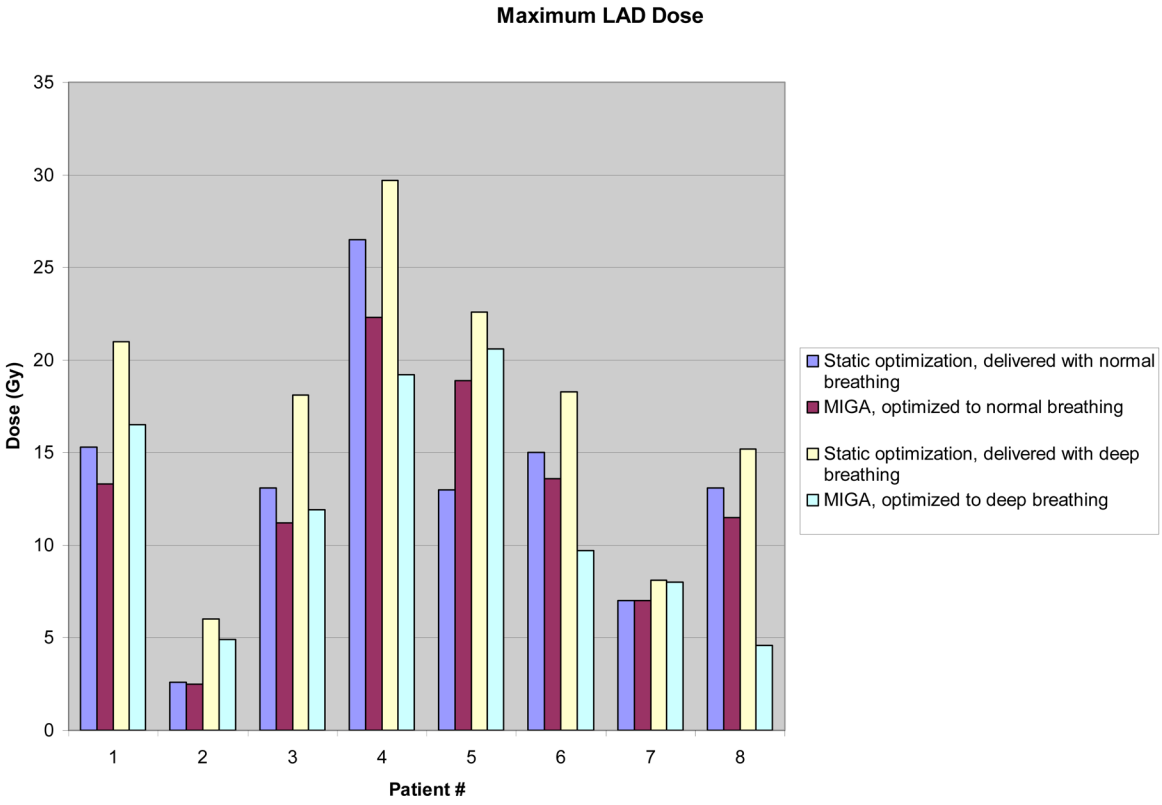

Figure 2.
Individual Patient Data for Maximum LAD Dose, comparing static vs MIGA-based optimization at both normal and deep breathing.
Abbreviations: LAD, Left Anterior Descending Artery; MIGA, Multiple Instance Geometry Approximation; Gy, Gray

Table 1

Dose Specifications and Planning Priorities

Priority	Target/Organ	Clinical Objective
1	Tumor bed PTV*	60 Gy to ≥ 99% of volume ≤1% of volume to exceed 63 Gy
	Breast PTV SCV§ and ICV† PTV IMN†† PTV	50.6 Gy to ≥ 99% of volume 52.2 Gy to ≥ 95% of volume ≤1% of volume to exceed 54.8 Gy 0% of volume to exceed 57.4 Gy
2	Heart and LAD[ ]	Maximum dose not to exceed 15 Gy Mean dose not to exceed 3 Gy
	Spinal cord	Maximum dose not to exceed 50 Gy Minimize overall dose
3	Contralateral breast and lung	Minimize dose. Limit to scatter dose. Beamlets forbidden to enter or exit through these structures
	Ipsilateral lung	≤30% of volume to exceed 30 Gy
4	Brachial plexus Carotid Artery Great Vessels	0% of volume to exceed 55 Gy Minimize overall dose

*Abbreviations:Planning Target Volume;

§Supraclavicular Lymph Nodes;

†Infraclavicular Lymph Nodes;

††Internal Mammary Lymph Nodes;

[ ]Left Anterior Descending Artery []¶#

Table 2

Analysis of dose distributions per optimized plan on different breathing states

Patient Intra- treatment Motion		Optimized Plans		
		Static-Exhale	MIGA*-Normal- Respiration	MIGA-Deep- Respiration
	Immobilized at End Exhale	X		
	Normal Respiration	X	X	
	Deep Respiration	X		X

*Abbreviations: Multiple Instance Geometry Approximation

Table 3

Comparison of average mean (or maximum) doses (Gy, ±σ), delivered with a static-based IMRT plan, with varying patient motion.

Target/OAR*	Dose (Gy) ± Standard deviation		
	Immobilized at End Exhale	Normal Respiration	Deep Respiration
Boost	60.4 ± 0.2	57.7 ± 7.0 (p = 0.31)	59 ± 2.5 (p = 0.14)
Breast	52.3 ± 1.4	50.2 ± 6.9 (p = 0.36)	51.5 ± 2.3 (p = 0.37)
SCV§	52.4 ± 0.9	52.6 ± 0.8 (p = 0.23)	52.6 ± 0.9 (p = 0.25)
ICV†	53.1 ± 0.5	53 ± 0.7 (p = 0.32)	52.6 ± 1.2 (p = 0.19)
IMN††	50.8 ± 3.9	48 ± 9.8 (p = 0.35)	49.8 ± 3.9 (p = 0.30)
Heart	0.7 ± 0.7	0.8 ± 0.8 (p = 0.10)	0.9 ± 0.9 (p = 0.04)
Heart (Max)	9.3 ± 8.4	10.8 ± 8.7 (p = 0.07)	13.5 ± 9.0 (p = 0.01)
LAD[ ]	2.5 ± 2.2	2.5 ± 2.0 (p = 0.89)	3.5 ± 2.4 (p = 0.003)
LAD (Max)	11.6 ± 7.6	13.2 ± 6.9 (p = 0.37)	17.4 ± 7.7 (p = 0.01)
Ipsilateral lung	11.9 ± 1.8	11.2 ± 2.6 (p = 0.53)	13 ± 2.1 (p = 0.04)

*Abbreviations: Organs at Risk;

§Supraclavicular Lymph Nodes;

†Infraclavicular Lymph Nodes;

††Internal Mammary Lymph Nodes;

[ ]Left Anterior Descending Artery

Table 4

Plan technique comparison for minimum and mean target coverage (Gy, ± σ), and dose to organs at risk, delivered at normal breathing.

Target/Organ at Risk		Dose (Gy) ± Standard deviation		P value
		Optimization to End Exhale	MIGA*-based optimization to normal breathing	
Breast	Minimum	17.2 ± 12.3	16.0 ± 11.4	0.13
	Mean	50.2 ± 6.9	52.3 ± 1.5	0.36
SCV§	Minimum	28.2 ± 12	28 ± 12	0.65
	Mean	52.6 ± 0.8	52.6 ± 0.8	0.68
ICV†	Minimum	33.4 ± 9.7	35 ± 6.7	0.59
	Mean	53.1 ± 0.5	53.3 ± 0.6	0.08
IMN††	Minimum	26.1 ± 14.3	26.2 ± 13.3	0.90
	Mean	48 ± 9.8	50.8 ± 4	0.30
Tumor Bed	Minimum	54.8 ± 9.1	57.1 ± 4	0.25
	Mean	57.7 ± 7	60.4 ± 0.3	0.31
Heart	Mean	0.8 ± 0.8	0.7 ± 0.8	0.89
	Maximum	10.8 ± 8.7	10.4 ± 9	0.58
LAD[ ]	Mean	2.5 ± 2	2.5 ± 2	1
	Maximum	13.2 ± 6.9	12.5 ± 6.2	0.55
Ipsilateral Lung		11.2 ± 2.6	11.9 ± 1.6	0.34

*Abbreviations: Multiple Instance Geometry Approximation;

§Supraclavicular Lymph Nodes;

†Infraclavicular Lymph Nodes;

††Internal Mammary Lymph Nodes;

[ ]Left Anterior Descending Artery

Table 5

Plan technique comparison for minimum and mean target coverage (Gy, ±σ), and dose to organs at risk, delivered with deep respiration

Target/Organ at Risk		Dose (Gy) ± Standard deviation		P value
		Optimization to End Exhale	MIGA*-based optimization for deep respiration	
Breast	Minimum	19.8 ± 12.3	14.3 ± 12.3	0.07
	Mean	51.5 ± 2.3	52.2 ± 1.4	0.46
SCV§	Minimum	28.8 ± 11.9	27.9 ± 11.9	0.36
	Mean	52.6 ± 0.9	52.6 ± 0.8	0.54
ICV†	Minimum	33.4 ± 10.5	36.8 ± 5.9	0.35
	Mean	52.6 ± 1.2	53.3 ± 0.5	0.11
IMN††	Minimum	28.8 ± 12.2	28.7 ± 12.8	0.94
	Mean	49.8 ± 3.9	51.2 ± 3.6	0.14
Tumor Bed	Minimum	55.4 ± 2.3	57.9 ± 2	0.04
	Mean	59 ± 2.5	60.5 ± 0.3	0.12
Heart	Mean	0.9 ± 0.9	0.7 ± 0.8	0.06
	Maximum	13.5 ± 9	10.5 ± 8.5	0.02
LAD[ ]	Mean	3.5 ± 2.4	2.6 ± 2	0.01
	Maximum	17.4 ± 7.7	11.9 ± 6.2	0.008
Ipsilateral Lung		13.0 ± 2.1	12.6 ± 1.6	0.39

*Abbreviations: Multiple Instance Geometry Approximation;

§Supraclavicular Lymph Nodes;

†Infraclavicular Lymph Nodes;

††Internal Mammary Lymph Nodes;

[ ]Left Anterior Descending Artery